

ON THE COMBUSTION KINETICS OF HETEROGENEOUS CHAR PARTICLE POPULATIONS*

R. H. Hurt and R. E. Mitchell**

Combustion Research Facility

Sandia National Laboratories, Livermore, CA 94551-0969

Keywords: coal, combustion, kinetics

An optical technique has previously been used to measure, *in situ*, the temperatures, sizes, and velocities of individual pulverized-coal char particles.¹⁻³ A model of mass and energy transport processes to and from the burning char particles was used to derive burning rates and kinetic parameters from the single-particle measurements. In the past, the measured joint distribution of particle temperature and size was divided into narrow size fractions, and global kinetic parameters were determined from the average temperatures and sizes in these fractions.^{2,3} An effort is currently underway to extract additional information from the existing extensive data base by computing and analyzing burning rates and rate coefficients for *individual* particles derived directly from the single-particle temperature measurements. In the present article, single-particle rate coefficients are computed from optical measurements on char from Pocahontas #3 coal†, and techniques for the determination of kinetic parameters from the single-particle coefficients are investigated.

RESULTS

A laboratory-scale laminar-flow reactor was used to investigate the combustion of Pocahontas #3 low-volatile bituminous coal particles (nominal diameter range 106 -124 μm) in gas environments containing 6 or 12 mole-% oxygen over the range of gas temperatures 1500 -1700 K. An optical particle sizing/pyrometer was used to measure single-particle temperatures, sizes, and velocities during the char combustion phase (subsequent to devolatilization). Char particle sizes differ from the nominal coal particle size due to both swelling during devolatilization and surface carbon consumption. A model of mass and energy transport processes was used to extract burning rates and kinetic parameters from the single-particle optical measurements. The model treats unsteady radiative and convective heat transfer between the particle and its surroundings as well as oxygen transport to the particle surface, accounting for the effect of Stefan flow. The principle and operation of the optical particle sizing/pyrometer and the transport model are discussed in detail elsewhere.¹⁻³ Char oxidation kinetics are represented here by a rate law of the form:

$$q = k_s P_s^n = A e^{(-E/RT_p)} P_s^n \quad (1)$$

where q is the burning rate per unit external particle surface area, and k_s is a global coefficient embodying the combined effects of internal surface area, pore diffusion, and intrinsic surface reactivity. The combustion behavior of a given coal char is described by the set of three global kinetic parameters, n (reaction order), E (activation energy), and A (preexponential factor).

Single-particle rate coefficients

At each measurement location in the flow reactor (i.e. at successive particle residence times), the optical technique recorded a distribution of particle sizes and temperatures. Standard deviations typically observed were 20 μm in particle diameter and 40 to 120 K.

* Work supported by the U.S. Department of Energy's Pittsburgh Energy Technology Center's Direct Utilization AR&TD Program.

** Present address: Department of Mechanical Engineering, Stanford University, Stanford, CA 94305-3032

†† The Pocahontas #3 coal was obtained from the Pennsylvania State Coal Bank (designation PSOC-1508), through the Pittsburgh Energy Technology Center, and is one in a suite of ten coals under study within the Sandia Coal Combustion Science Program.

in particle temperature. In Figure 1, single-particle rate coefficients derived from the optical data on Pocahontas #3 coal, are plotted as a function of temperature, in Arrhenius form[†]. A characteristic feature of this and other Arrhenius plots of single-particle rate constants is the presence of distinct linear groupings of points associated with a given gas composition and a given measurement location in the reactor. These linear groupings generally exhibit slopes that are steeper than the kinetic rate expression fit to the entire data set. As a result of this feature, data taken in only a single gas environment (e.g. 12-mole% O₂) produce activation energies generally higher than those determined from a simultaneous regression of data in several gas conditions.⁴

In Figure 2, single-particle rate constants are plotted for the same data set, but for the optimum (least squares) reaction order, $n = 0.0$. By varying the reaction order, the data from Fig. 1 have been partially collapsed to a single curve. Experience with similar data for a number of coals indicates that it is often possible to find a reaction order that at least partially collapses the data from different measurement locations. For some data sets, however, no value of n collapses the data onto one curve, resulting in a kinetic expression (a set of values for n , E , and A) that does not adequately describe the entire data set. In either case, the basic trend toward collections of distinct lines with higher slopes is apparently an intrinsic property of Arrhenius plots of single particle combustion rate constants. The origin of this feature will be explained in the next section.

DISCUSSION

Characteristic curves on Arrhenius diagrams

Let us consider a simplified analysis that ignores the effect of Stefan flow (a minor correction) and assumes the particles to be in thermal equilibrium with their environment. Under these conditions, given a reaction order n , the equations governing mass and energy transport can be algebraically manipulated to arrive at the following explicit expression for the single-particle rate constant, k_s .

$$k_s = \left[\frac{\frac{Nu\lambda}{H_{rxn}d_p}(T_p - T_g) + \frac{\epsilon_p\sigma}{H_{rxn}}(T_p^4 - T_w^4)}{P_g - \frac{d_p R(T_p + T_g)}{48D_{ox}} \left(\frac{Nu\lambda}{H_{rxn}d_p}(T_p - T_g) + \frac{\epsilon_p\sigma}{H_{rxn}}(T_p^4 - T_w^4) \right)} \right]^n \quad (2)$$

From Eq. 2 k_s is a function of the following variables: T_p , d_p , T_g , P_g , T_w , n , D_{ox} , λ , ϵ_p , H_{rxn} . For a given operating condition at a given measurement height, T_p and P_g are fixed, as are T_w and the properties of the gas D_{ox} and λ , and the heat of reaction, H_{rxn} . For coal particles with an emissivity ϵ_p , k_s is a function only of T_p , d_p , and n . If one fixes the reaction order, n , and considers only particles of a given size, d_p , Eq. 2 reduces to a relationship between T_p (which is measured in the laboratory) and k_s , (the derived quantity of interest, the single-particle rate coefficient). In a plot of k_s as a function of $1/T_p$, Eq. 2 defines a characteristic curve representing the mass and energy balances for the reacting char particle.

An example of such a characteristic curve is the leftmost trace in Fig. 3, calculated for the specific case: $d_p = 150 \mu\text{m}$, $\epsilon_p = 0.8$, $T_g = 1645 \text{ K}$, and $P_g = 0.12 \text{ atm}$ (corresponding to the 12.7 cm measurement height in the laminar flow reactor in the 12 mole-% O₂ gas environment). It is important to note that the characteristic curves are functions of the reaction order, n , but not of the other kinetic parameters, A and E . Also in Fig. 3 are data points corresponding to the 140-160 μm size fraction (a subset of the data in Fig. 1),

[†] Single-particle rate coefficients can be calculated from the optical data directly if the reaction order, n , is specified. A value for the reaction order of 1/2 was chosen arbitrarily for this example. Also, the results presented in Figures 1 - 4 were generated by a simplified analysis technique which assumes that CO is the only combustion product and that the particles are in thermal equilibrium with their environment.

superimposed on the theoretically derived characteristic curves for $d_p = 150 \mu\text{m}$. This particular linear grouping from Fig. 1 is seen to lie, as it must, along a characteristic curve representing the mass and energy balance equations for reacting char particles. The characteristic curves have the following features: at low particle reactivity (low k_s) the burning rate is insufficient to generate enough heat to affect the particle temperature - the temperature in this "nonburning" regime is nearly independent of k_s (see the nearly vertical curve segments at the bottom of Fig. 3), and accurate values of k_s cannot be extracted from the measured particle temperatures. For moderate particle reactivity (moderate k_s), the surface reaction generates sufficient heat to raise the particle temperature well above the nonburning temperature. In this region particle temperature is sensitive to k_s and the burning rates and kinetic parameters can be derived from the measured particle temperatures (see the sloped portion of the curves in the center of Fig. 3). At high particle reactivity (high k_s), particles burn so rapidly that oxygen is thoroughly depleted at the particle surface and an asymptotic temperature is reached associated with diffusion-limited or zone III burning. In this region the temperature again becomes insensitive to k_s , and extraction of accurate values of k_s from measured particle temperatures is no longer possible (see the vertical curve segments at the top of Fig. 3).

The characteristic curves exhibit many of the same features as plots of k_s vs. χ used by Smith⁵, where χ is the ratio of the observed burning rate to the maximum, diffusion-limited rate. Data points that lie in the nearly vertical upper or lower segments of the characteristic curves correspond to high and low values of χ respectively. For the determination of the kinetic parameters, only values within a chosen χ range (typically $0.2 < \chi < 0.85$) are used, corresponding to points that lie on the central, nearly linear segment of the curves.

Families of characteristic curves for a particle size distribution

It was shown in the previous section that rate constants, k_s , for individual burning particles of a given size, d_p , lie on characteristic curves on the Arrhenius diagram representing mass and energy balance equations for the reacting particles. In practice, even though size-graded coal is fed to the reactor, the devolatilization process broadens the particle size distribution to such an extent that the size dependence of char reactivity must be considered.

In Fig. 4 characteristic curves are presented for various particle sizes at two selected experimental conditions. Also appearing on Fig. 4 are single-particle rate constants for all particle sizes from Fig. 1, superimposed on the characteristic curves. The figure illustrates how a distribution of particle sizes at a given measurement height gives rise to a family of characteristic curves on the Arrhenius diagram. The range of particle sizes considered ($100 - 200 \mu\text{m}$) produces, for each condition, a band that contains essentially all of the measured points. There is a significant size dependence in the upper and lower extremes of the curves due to the size dependence in the convective mass and heat transfer coefficients in Eq. 2. In the central region, however, from which kinetic data are extracted, particle temperatures are only weakly size dependent and the family of curves converges to a narrow band. The measured rate constants (points) are therefore seen to lie in nearly linear groupings within the narrow bands formed by the nearly linear segments of the characteristic curve families.

It can therefore be concluded that the distinct linear groupings clearly seen in Arrhenius plots of single-particle rate constants are the outlines of the nearly linear sections of characteristic curves, with the particle size distribution causing a limited scatter about a central curve corresponding to the median particle size. These linear groupings of points, like the theoretical characteristic curves they follow, are a function of the reaction order, n , but not the actual global kinetic activation energy E or preexponential factor, A . The global kinetic activation energy and preexponential factor determine, rather, where along these curves the measured points will lie.

Implications for kinetic studies

With this background on characteristic curves, let us consider how kinetic parameters can be extracted from measurements of single-particle sizes and temperatures. A large number of single particle temperatures are measured and the model (represented here by a series of characteristic curves) is used to determine a value of k_s for each particle. As a consequence of the analysis procedure, each point on the Arrhenius diagram corresponding to a single-particle measurement from the laboratory must lie on one of the characteristic curves. This is true irrespective of the accuracy in the data - random measurement errors cause the data not to scatter *about* the characteristic curves, but to distribute *along* characteristic curves.

If kinetics are to be measured for a system in which each particle obeys a single rate law, for example the Arrhenius law, the individual data points will be the intersections of the line representing the Arrhenius rate law (Eq. 1) and the appropriate characteristic curve representing the particle mass and energy balance equations (Eq. 2). Because these curves intersect at only one point, there is only one particle temperature and one value of k_s that satisfy both the rate law and the mass and energy balances. The rate expression obtained by regression of the data will be a locus of experimental points lying on different characteristic curves.

In practice, particle-to-particle variations in properties and reactivity result in a distribution of particle temperatures at each location, producing a distribution of points along a characteristic curve, appearing as a distinctly recognizable line of slope $\beta = d(\ln k_s)/d(1/T_p)$. From the definition of the activation energy:

$$E \equiv -R \frac{d \ln k_s}{d(1/T_p)} \quad (3)$$

it is clear the the data at one experimental condition exhibit a pseudo activation energy of $-R\beta$. The slope, β , is a property of the associated characteristic curve and can be obtained by direct differentiation of Eq. 2. Examination of Eq. 2 reveals that this pseudo activation energy, $-R\beta$, associated with a given reactor height, is a function of T_p , d_p , T_g , P_g , n , T_w , D_{O_2} , λ , ϵ_p , and H_{rxn} .

The pseudo activation energy for data from a single measurement location is therefore a function of the reaction order, properties of the gas phase, and physical properties of the char particle, *but is independent of the actual global kinetic activation energy, E* . From this we can conclude that the temperature distribution observed in a given experiment at a single measurement location contains little or no information on the activation energy.[†] It is primarily in the comparison of data points taken at different measurement locations that the true information on the pressure dependence (n) and the temperature dependence (E) of the char combustion rate lies.

When a single Arrhenius rate law is fit to all experimental points simultaneously, optimal (least-squares) coefficients are influenced by particle-to-particle variations in properties and reactivity, manifested in the presence of the characteristic curve segments of generally higher slope. The regression routine attempts, in effect, to fit both the true kinetics and the characteristic curve segments simultaneously. The least-squares parameters obtained will be influenced both by the kinetic parameters (A, E, n), and by the properties of the characteristic curves. In practice, the presence of the linear groupings of single-particle rate coefficients affects the data regression in the following manner: Both the characteristic curves and their derivatives are functions of n , the reaction order. A comparison of Figs. 1 and 2 illustrate that the slope, and thus the pseudo activation energy at one height, tends to decrease with increasing n . Extraction of a rate law by regression of the entire set of single-

[†] Limited kinetic information is contained in the observed dependence of temperature on particle size at one measurement location.

particle data often results in artificially low reaction orders, because low orders produce characteristic curves of lower slope that are more closely comparable to typically observed activation energies for oxidation of impure carbons (typically 15 - 25 kcal/mole in zone 2). A parameter set (A, E, n) with low n partially collapses the data onto nearly parallel, closely spaced characteristic curves, resulting in a lower RMS error (see Fig. 2).

The extent to which particle-to-particle variation in properties and reactivity influences the kinetic parameters can be seen by repeating the analyses for Figs. 1 and 2 with data sets formed by various temperature averaging strategies. Table 1 presents the results of applying an identical analysis technique to three different data sets derived from the original measurements of single particle temperatures, sizes, and velocities for Pocahontas #3 coal:

1. individual particle sizes and temperatures
2. average sizes and temperatures in 10 μm size bins
3. overall median particle sizes and temperatures at each experimental condition and measurement location.[†]

An optimal value of the reaction order was determined by minimizing the sum of the squared residuals in k_p . Table 1 shows a sharply increasing value of n with an increasing degree of temperature averaging. Averaging decreases the amount of scatter along characteristic curves and thus reduces the biasing effect on the kinetic parameters. The use of average temperatures in 10 μm size bins reduces the length of the characteristic curve segments and thus reduces the biasing effect, but does not eliminate it. Use of the overall median values, corresponding to a reaction order of 0.75, is believed to yield unbiased results for this data set.

Recommended Technique for Determination of Kinetic Parameters

The distribution of particle temperatures at one measurement location reflects the effects of particle size and of particle-to-particle variations in both physical properties and reactivity. For the Pocahontas coal char the effect of variations in particle size is quite small. To understand the origin and evolution of the observed temperature distributions, a more detailed statistical treatment is needed that explicitly considers particle-to-particle variations in both physical properties and reactivity. Gavalas and Flagan⁶ have used a statistical model of char combustion to describe variability in temperature traces of individual burning coal particles.

For the more limited practical goal of predicting overall burning rates for the particle population over narrow to moderate ranges of carbon conversion, kinetic parameters describing the combustion behavior of "typical" particles in the population (those of median reactivity) is often sufficient. It has been shown here, that even this limited goal cannot be attained by direct application of nonstatistical analyses to single-particle measurements. The presence of the particle temperature distributions has been shown to introduce a systematic bias in the determination of kinetic parameters, resulting for this example, in artificially low reaction orders. In the following paragraphs, a simple analysis technique is recommended that avoids this bias and yields kinetic parameters describing the combustion of "typical" particles within a heterogeneous particle population.

In general, the joint size/temperature distribution measured by the single-particle optical technique contains valuable information on the kinetic parameters A, E , and n . There is, however, often a wide variation in temperature within a particle size fraction, which has been shown to systematically bias kinetic analyses. Classifying the single-particle data into narrow size bins preserves much of the information in the T_p - d_p relationship, but produces average temperatures for each size bin that are based on few data points. The averages therefore contain a significant fraction of the scatter present in the original temper-

[†] These three optimum reaction orders were determined by a kinetic analysis that assumed CO to be the only combustion product, but accounted for the influence of particle thermal inertia on the heat balance (a term arises for thermal inertia when the particles traverse regions of changing gas temperature or properties).

ature distribution, according to Eq. 4:

$$\sigma_{T_{ave}} = \sigma_T / \sqrt{N} \quad (4)$$

where σ_T is the standard deviation in the measured temperature distribution and $\sigma_{T_{ave}}$ is the standard deviation of the averages computed from N experimental points. Wide size bins, on the other hand, produce accurate estimates of the average temperatures (reducing the bias associated with the distinct lines) but sacrifice much of the information contained in the T_p - d_p dependence. For a given experiment, there is an optimum width for the size bins that results in the most accurate determination of the kinetic parameters A , E , and n .

A simple statistical technique for determination of n^{th} -order kinetic parameters was developed and used that achieves the proper balance between temperature averaging and preservation of information contained in the joint size/temperature distribution. The single-particle data was divided into only two size categories: one containing particles between the 0th - 50th size percentiles (with a median at the 25th percentile) and a second containing particles between the 50th - 100th size percentiles (with a median at the 75th). Median sizes and temperatures are obtained for each of the two categories by a sorting routine and are combined with the overall median size and temperature to yield the data set for regression. Rate parameters for the Pocahontas coal determined by the technique outlined above are presented in Fig. 5. The full analysis of Mitchell³, including the effects of thermal inertia, Stefan flow, and partial CO₂ production at the particle surface was applied. The reaction order was determined to be 0.75 by least squares regression and the CO/CO₂ ratio was adjusted to fit the measured mass-loss profiles using the correlating expression $CO/CO_2 = A_c e^{(-E_c/RT)}$. Inclusion of some CO₂ production improves the fit to the conversion profile and average values of ψ , the fractional molar conversion to CO₂, are reported in Fig. 5 for the two gas environments (6, 12 mole-% oxygen).

CONCLUSIONS

Particle-to-particle variations in properties and reactivity often give rise to a broad distribution of char particle temperatures at a given location in a combustion environment. This distribution of particle temperatures is shown to produce distinct characteristic curves or bands of points on Arrhenius plots of single-particle rate constants. These linear features exhibit pseudo activation energies that are independent of the actual global kinetic activation energy. A complete description of single-particle combustion behavior will require a detailed statistical treatment that explicitly accounts for the origin and implications of the observed temperature distributions. Accounting for particle-to-particle variations in reactivity and properties may be key to understanding reactivity at high carbon conversions. For the more limited goal of predicting overall burning rates for the entire particle population over narrow to moderate ranges of carbon conversion, kinetic parameters describing the combustion behavior of "typical" particles (those of median reactivity) is often sufficient. It has been shown here, that even this limited goal cannot be attained from single particle measurements without careful statistical considerations. The observed particle-to-particle variations in properties and reactivity are shown to dramatically bias the global kinetic parameters determined by nonstatistical analysis. A simple analytical procedure is demonstrated that extracts the true kinetic information for particles of median reactivity within a heterogeneous particle population.

LITERATURE

1. Tichenor D. A., Mitchell R. E., Hencken K. R., and Niksa S. 20th Symp. (Int.) Comb. 1213 (1984)
2. Mitchell, R. E. and Madsen, O. H. 21st Symp. (Int.) Comb. 173 (1986)
3. Mitchell, R. M. 22nd Symp. (Int.) on Comb., 69 (1988)
4. Mitchell, R. M., and D. R. Hardesty, in *Coal Combustion Science—Quarterly Progress Report*, Hardesty, D. R. (ed.), Sandia Report SAND89-8250 (1989).
5. Smith, I. W., 19th Symp. (Int.) on Comb. 1045 (1982)
6. Gavalas, G. R. and Flagan, R. C. "Kinetics of Coal Combustion Part III: Mechanisms and Kinetics of Char Combustion," Final Report to the Dept. of Energy, Rpt.# TRW S/N 44617

NOMENCLATURE

A	preexponential factor	R	gas constant
A_c	preexponential factor in the correlation for CO/CO ₂ ratio	T_g	gas temperature
d_p	particle diameter	T_p	particle temperature
D_{ox}	oxygen diffusivity	T_w	wall temperature
E	global kinetic activation energy for char oxidation	v_g	gas velocity
E_c	activation energy in the correlation for CO/CO ₂ ratio	v_p	particle velocity
H_{eff}	heat of combustion reaction	Greek Symbols	
k_s	rate constant	β	slope of characteristic curve
n	reaction order	ϵ_p	particle emissivity
P_g	partial pressure of oxygen in the bulk gas	λ	thermal conductivity of the gas phase
P_s	partial pressure of oxygen	Nu	Nusselt number
q	burning rate per unit area of external surface	σ	Stefan-Boltzmann constant
		σ_T	standard deviation of measured temperature
		$\sigma_{T_{ave}}$	standard deviation of average temperature
		χ	ratio of observed to maximum burning

**Table 1. Optimum Reaction Order for Oxidation of PSOC-1508 Char
Determined From Three Different Data Sets**

<i>Data Set used in Regression</i>	<i>Reaction order</i>
All single-particle sizes and temperatures	0.00
Average sizes and temperatures in 10 μm size bins	0.16
Overall median sizes and temperatures	0.75

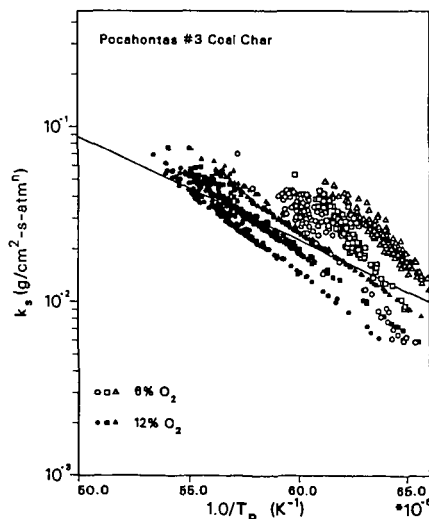


Figure 1. Rate constants for individual burning char particles from Pocahontas #3 (PSOC-1508) coal: Reaction order, $n_s = 1/2$. Initial coal particle diameters 106 - 125 μm . Reaction product assumed to be CO. Symbols correspond to various measurement heights (particle residence times): circles: 12.7 cm; squares: 19.1 cm; triangles 25.4 cm.

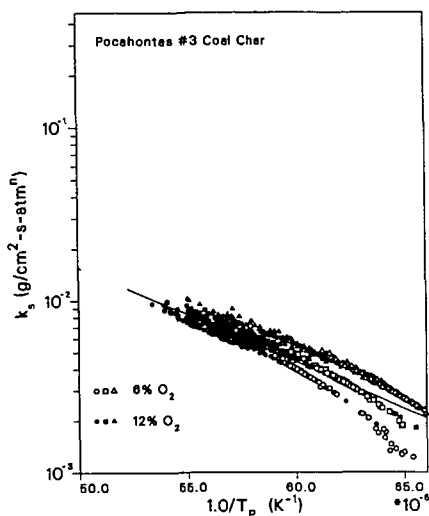


Figure 2. Rate constants for individual burning char particles from Pocahontas #3 (PSOC-1508) coal: optimum reaction order, $n = 0.0$. Initial coal particle diameters 106 - 125 μm . Reaction product assumed to be CO. Symbols correspond to various measurement heights (particle residence times): circles: 12.7 cm; squares: 19.1 cm; triangles 25.4 cm.

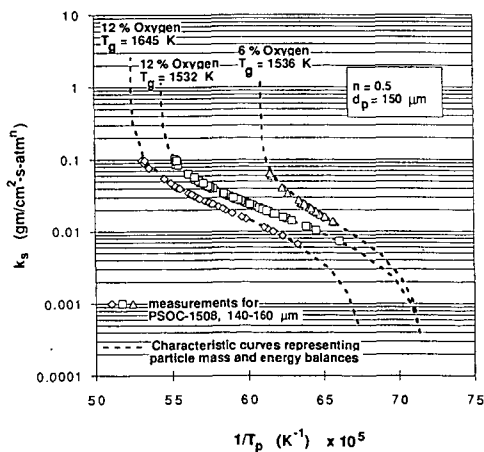


Figure 3. Characteristic curves and experimentally determined single-particle rate constants for PSOC-1508 Pocahontas #3 coal. Curves for 150 μm particles; points for particles with diameters 140 - 160 μm . Reaction order, $n = 1/2$.

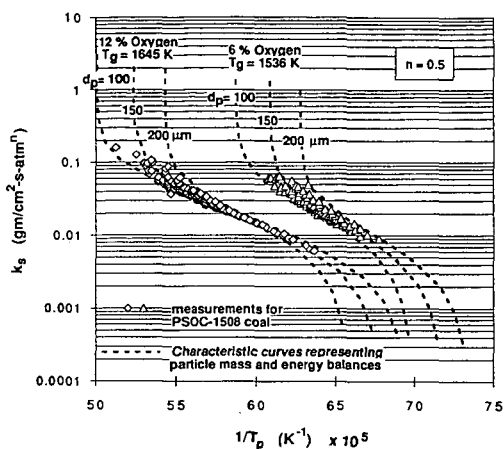


Figure 4. Families of characteristic curves for a particle size distribution and experimentally determined single-particle rate constants for PSOC-1508. Reaction order, n , = 1/2.

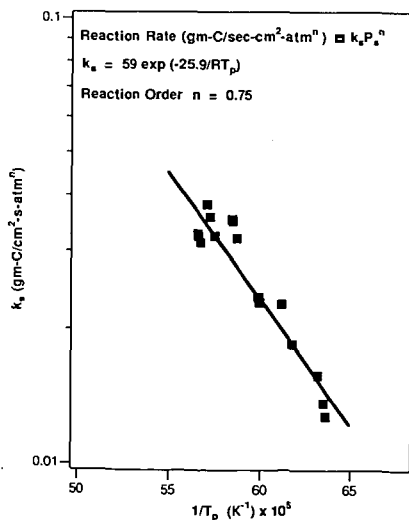


Figure 5. Global kinetic parameters for PSOC-1508 Pocahontas #3 low-volatile bituminous coal. Points represent rate coefficients calculated by the recommended simple statistical technique.